Int. J. Electrochem. Sci., 17 **(2022)** Article Number: 221279, doi: 10.20964/2022.12.76

International Journal of
ELECTROCHEMICAL
SCIENCE
www.electrochemsci.org

Analytical Detection of Hepatitis B Antiviral Drug Entecavir using Hemoglobin Modified Nitrogen-Doped Carbon Nanotube Sensor

Junqiu Jiang[1], *Feng Ren*[2,*]

[1] Pharmaceutical Department, The Second Affiliated Hospital of Dalian Medical University, Dalian, Liangning Province, PR China
[2] Department of Laboratory Medicine, The Second Affiliated Hospital of Dalian Medical University, Dalian, Liangning Province, PR China
[*]E-mail: dyarenfeng@126.com

Received: 2 October 2022 / *Accepted:* 22 November 2022 / *Published:* 27 December 2022

Entecavir is the first-line drug for the treatment of hepatitis B. However, at this stage, there is no very mature technique for the rapid detection of entecavir. In this work, a novel electrochemical biosensor for entecavir was constructed using highly conductive nitrogen-doped carbon nanotubes as a solid-loaded substrate and hemoglobin as a recognition element. The experimental results showed that the electrochemical performance of the sensor was better than that of the nitrogen-doped carbon nanotubes with the incorporation of hemoglobin, which showed good linearity in the detection range of 10-100 μM with a detection limit of 4.38 μM (S/N=3). In addition, the electrochemical sensor showed excellent performance when applied to actual samples of serum and urine for the detection of entecavir.

Keywords: Electrochemical sensor; Entecavir; Nitrogen-doped carbon nanotubes; Hemoglobin; Serum

1. INTRODUCTION

More than 2 billion people worldwide are currently infected with hepatitis B virus (HBV), and approximately 350 million are chronically infected. Cirrhosis, liver failure, and primary hepatocellular carcinoma caused by HBV infection result in approximately one million deaths per year [1]. Hepatitis B virus carriers of which enter the chronic liver disease stage account for 25%, leading to cirrhosis, chronic hepatitis and liver cancer [2,3]. This process can be slowed or stopped by effective treatment against the hepatitis B virus. Interferons and nucleosides are the two major classes of internationally recognized antiviral therapeutic agents, of which nucleosides are orally administered, convenient and universally preferred [4,5]. Entecavir was first approved by the U.S. FDA in March 2005 under the trade name

"Baraclude". It is the first HBV-specific antiviral drug that is non-cross-reactive with HIV and herpes viruses. According to the consensus from the 2008 Asia Pacific Liver Conference, lamivudine is no longer the drug of choice for patients with rapidly increasing resistance rates among long-term users, while entecavir is becoming the drug of choice for antiviral therapy because of its high efficiency and very low resistance rate [6–9].

Currently, the most commonly used methods for the detection of entecavir are ion chromatography, gas chromatography, and liquid chromatography [10–17]. These methods have high accuracy and sensitivity, but there are limitations such as large size of instrumentation, high requirements for operators, complex and time-consuming sample pre-treatment, and high costs, which are not conducive to rapid analysis and emergency detection of entecavir. Detection methods for entecavir also include UV-Vis spectrophotometry, chemiluminescence, fluorescence spectrometry and electrochemical analysis [18–25]. Among them, electrochemical analysis has been widely concerned due to the advantages of easy operation, low cost, fast detection speed and high sensitivity. Based on electrochemical sensing technology, it is expected to develop new methods for highly sensitive and rapid detection of entecavir, and to develop new portable devices that can be applied to both laboratory and field rapid detection.

In this study, an electrochemical biosensor was constructed based on the high electrical conductivity, high specific surface area and biocompatibility of nitrogen-doped carbon nanotubes (NCNT), and the specific recognition of entecavir by hemoglobin (Hb). The electrochemical behavior of entecavir at the modified sensing interface was investigated to examine the key properties of the sensor such as sensitivity, detection limit, selectivity and reproducibility of entecavir detection. This work proposes a new method for the highly sensitive, selective, rapid screening and quantitative detection of entecavir.

2. EXPERIMENTAL

2.1. Chemicals and instruments

Nitrogen-doped carbon nanotubes (NCNT) were purchased from Dalian Institute of Chemical Physics. Chitosan (CS, ≥75% deacetylation) was purchased from Sigma Aldrich (Shanghai). $Na_2HPO_4 \cdot 12H_2O$, $NaH_2PO_4 \cdot 2H_2O$, $K_3Fe(CN)_6$, $K_4Fe(CN)_6 \cdot 3H_2O$, KCl were purchased from Sinopharm. Entecavir was purchased from Anhui Baker United Pharmaceutical Co.

CHI660E electrochemical workstation was purchased from Shanghai Chenhua Instrument Co. KQ3200DE CNC ultrasonic cleaner was purchased from Kunshan Ultrasonic Instrument Co. PHS-3C pH acid meter was purchased from Shanghai Precision Scientific Instrument Co. Bruker D8 ADVANCE powder X-ray diffractometer (XRD, BRUKER, Germany) was used for XRD pattern collection.

2.2. Preparation of sensors

Polishing glassy carbon electrode (GCE): the GCE was polished to mirror surface with 1, 0.3, 0.05 μm Al_2O_3 powder in turn, then ultrasonically cleaned in ultrapure water and anhydrous ethanol, and blown dry with high purity N_2.

Preparation of hemoglobin-nitrogen-doped carbon nanotube sensors (Hb-NCNT-Chi/GCE): The Hb-NCNT-CS complex was prepared at concentrations of 2.5, 0.25 and 1.5 mg/mL for Hb, NCNT and CS, respectively. 5 μL of the above complex was applied to the newly polished GCE surface and left to dry at room temperature to obtain Hb-NCNT-CS/GCE. GS/GCE was prepared by a similar method but the complex did not contains Hb and NCNT. Hb-CS/GCE was also prepared by a similar method but the complex did not contains NCNT.

2.3. Detection of entecavir

A three-electrode system was used for electrochemical testing: a modified pole GCE (3 mm) as the working electrode, an Ag/AgCl electrode (KCl concentration of 3 M) as the reference electrode, and a platinum electrode as the counter electrode. For the cyclic voltammetry (CV) detection of entecavir, a phosphate buffer solution (PBS, pH 5.0, 50 mM) was used as the electrolyte solution with a scan rate of 50 mV/s. The electrochemical impedance spectroscopy (EIS) was performed under a 1 mM $K_3[Fe(CN)_6]/K_4[Fe(CN)_6]$ solution (containing 0.5 M KCl) as the supporting electrolyte. The frequency sweep range was 0.1 ~ 10000 Hz with an amplitude of 10 mV. All electrochemical tests were performed at room temperature.

3. RESULTS AND DISCUSSION

From the SEM image (Figure 1A), it can be seen that NCNT is a one-dimensional tubular structure with a diameter of about 15 nm. The XRD patterns in Figure 1B show that the NCNT shows the diffraction peaks of 002 and 111 graphite crystal phases at 26.0° and 42.9°, respectively, indicating that the NCNT has a clear graphite layer structure [26,27].

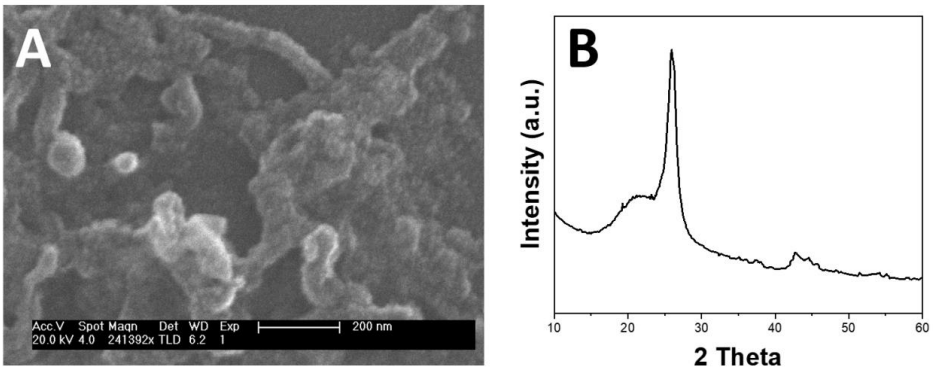

Figure 1. (A) SEM image and (B) XRD pattern of NCNT.

Figure 2 shows the electrochemical impedance plots of different modified electrodes (Nyquist plot, CHI660E electrochemical workstation) with the order of the impedance values: Hb-CS/GCE > Hb-NCNT-CS/GCE > CS/GCE > bare GCE. it can be seen from Figure 3 that the bare GCE and CS-GCE are almost in a straight line, indicating that the electrode has a very fast electron transfer rate with $[Fe(CN)_6]^{3-/4-}$ is very fast [28]. When Hb was added to the chitosan, the semicircular part increased significantly, indicating that the poorly conducting Hb had been modified to the electrode. With the addition of NCNT, the impedance becomes significantly smaller, indicating that the highly conductive NCNT greatly facilitates the electron transfer rate between the modified electrode and $[Fe(CN)_6]^{3-/4-}$, which significantly improves the conductivity of the sensor [29].

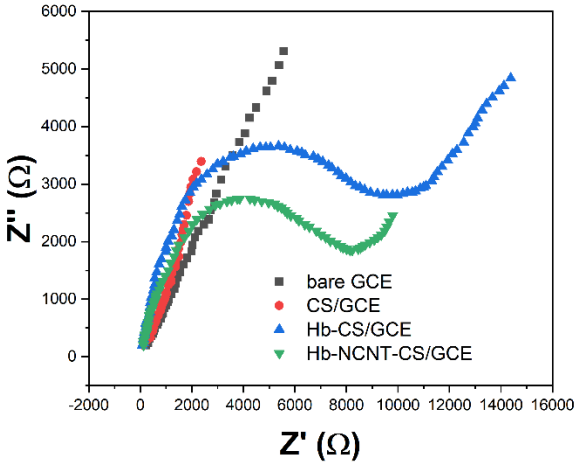

Figure 2. EIS of bare GCE, CS/GCE, Hb-CS/GCE and Hb-NCNT-CS/GCE in $[Fe(CN)_6]^{3-/4-}$.

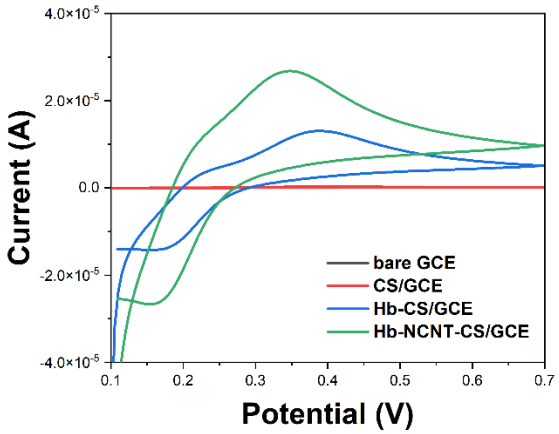

Figure 3. CV curves of bare GCE, CS/GCE, Hb-CS/GCE and Hb-NCNT-CS/GCE in PBS (pH=7) containing 0.1 mM entecavir.

We used cyclic voltammetry (CV) to investigate the electrochemical response of different modified electrodes to entecavir at a scan rate of 0.1 V/s. The measured voltage range was from 0.1 to 0.7 V. The test solution was 0.1 mM entecavir in 0.1 M PBS (pH=7). Scans were performed using bare GCE, CS/GCE, Hb-CS/GCE and Hb-NCNT-CS/GCE through CV, respectively, and the results are shown in Figure 3. The redox peaks appearing on the bare electrode GCE are not obvious. There is also no obvious signal response for CS/GCE. Hb-CS/GCE electrode has a slightly obvious electrochemical response, but the signal intensity is far inferior compared to Hb-NCNT-CS/GCE [30,31]. This indicates a better response of the Hb-NCNT-CS/GCE electrochemical sensor for entecavir detection.

The electrochemical response behavior of entecavir on Hb-NCNT-CS/GCE electrode was probed by DPV to detect the pH of PBS buffer solution as shown in Figure 4. The results showed that the peak current of entecavir increased with increasing pH as the pH of the buffer solution was increased from 4 to 7. During the increase of pH from 7 to 9, it decreased with the increase of pH. The peak current was maximum at pH 7 of the buffer solution, so we took the PBS buffer solution with pH 7 for the next electrochemical experiments.

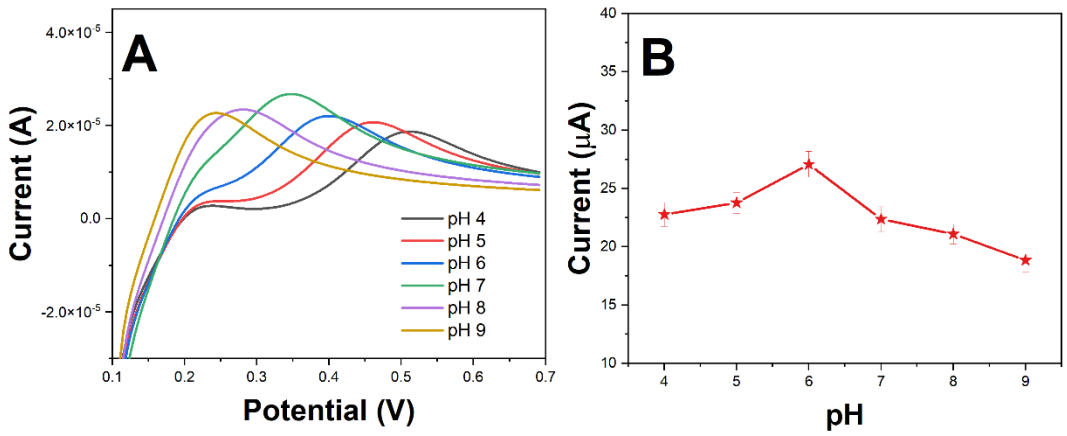

Figure 4. (A) DPV curves and (B) current plots of Hb-NCNT-CS/GCE in PBS towards 0.1 mM entecavir.

DPV is characterized by high sensitivity and low detection limits. Under optimal conditions, we explored the relationship between entecavir concentration and current. As shown in Figure 5, the entecavir oxidation peak current increased linearly with entecavir concentration from 10 μM to 100 μM. The linear measurement range was from 10 to 100 μM. linear correlation: I (μA) = 0. 11 C (μM) + 16.214 (R^2 = 0.9914). The detection limit of the electrochemical sensor for entecavir was 4. 38 μM at a triple signal-to-noise ratio. The detection limit of the sensor was not the lowest compared to other reports in the literature [32,33], but it still has a good application. This is because the electrochemical oxidation behavior of Entecavir has a relatively large broad peak rather than a sharp narrow peak. At the same time, its electrochemical activity is not very outstanding. Therefore, its detection sensitivity is difficult

to reach the ideal state. We are further optimizing the detection system and electrode materials, hoping to further improve the sensitivity of the sensor in the future work.

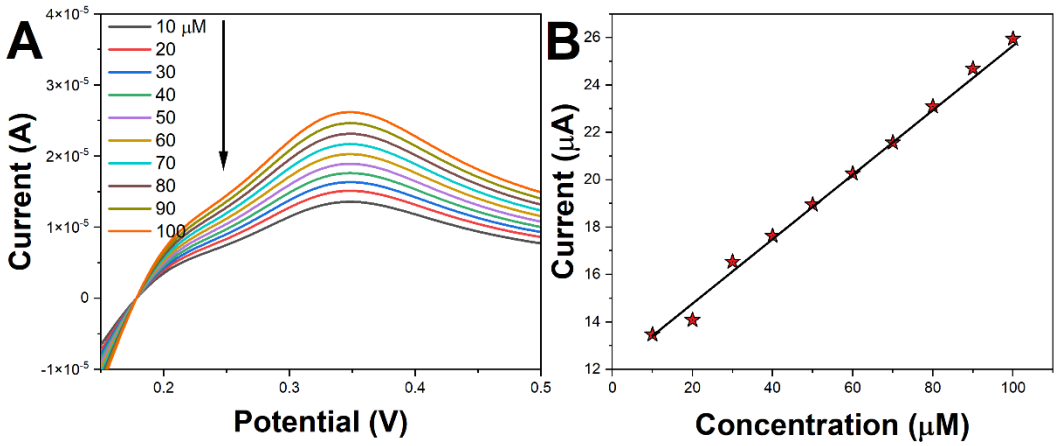

Figure 5. (A) DPV curves and (B) current plots of Hb-NCNT-CS/GCE in PBS towards 10 μM-100 μM entecavir.

Reproducibility and stability of electrochemical sensors are important indicators of good or bad sensors. In Figure 7A, five modified electrodes prepared under the same conditions were selected for the electrochemical detection of entecavir with a relative standard deviation (RSD) of 3.51%, and the sensor had good reproducibility. To investigate the stability of the electrochemical sensor, 0.1 mM entecavir was intermittently tested every five days, as shown in Figure 7B, and the response signal was 96. 1% of the initial signal value by 25 days of testing. The experiments also showed that the sensor was reproducible and stable.

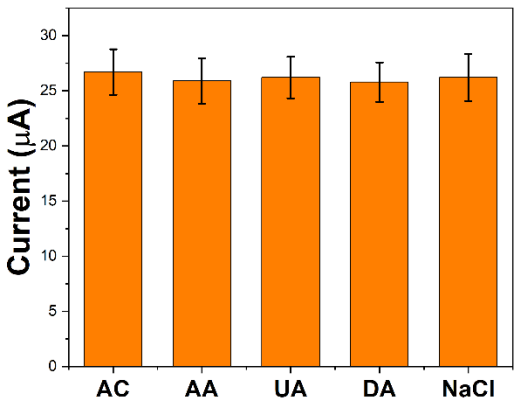

Figure 6. Anti-interference property of Hb-NCNT-CS/GCE towards entecavir in the presence of AA, UA, DA, NaCl.

Reproducibility and stability of electrochemical sensors are important indicators of good or bad sensors. In Figure 7A, five modified electrodes prepared under the same conditions were selected for the electrochemical detection of entecavir with a relative standard deviation (RSD) of 3. 51%, and the sensor had good reproducibility. To investigate the stability of the electrochemical sensor, 0.1 mM entecavir was intermittently tested every five days, as shown in Figure 7B, and the response signal was 96. 1% of the initial signal value by 25 days of testing. The experiments also showed that the sensor was reproducible and stable.

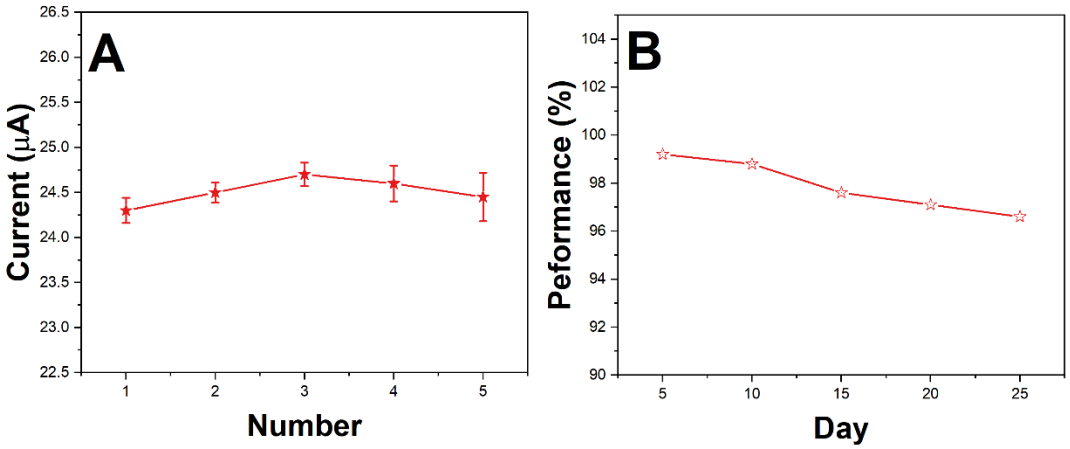

Figure 7. (A) Reproducibility and (B) stability of the Hb-NCNT-CS/GCE towards 0.1 mM entecavir.

In order to evaluate the practicality of the constructed electrochemical sensor, the concentration of entecavir in the serum and urine was determined using the standard addition method under optimal experimental conditions. As shown in Table 1, the recovery of entecavir in serum samples ranged from 99. 10% to 102. 10% (n=5) and in urine samples from 97.14% to 106. 15 % (n=5), indicating that the electrochemical sensor has a good performance in the detection of real samples.

Table 1. Determination of entecavir in actual samples using Hb-NCNT-CS/GCE

Sample	Addition	Detection	Recovery (%)	RSD (%)
Serum	10.00 μM	10.22 μM	102.20	4.22
	20.00 μM	21.23 μM	106.15	1.78
	50.00 μM	48.57 μM	97.14	2.05
Urine	10.00 μM	9.89 μM	98.90	3.01
	20.00 μM	21.09 μM	105.45	1.86
	50.00 μM	51.88 μM	103.76	3.05

4. CONCLUSION

A novel electrochemical biosensor was constructed for the detection of entecavir using the high electrical conductivity of nitrogen-doped carbon nanotubes and the specific catalytic reduction of hemoglobin.Hb-NCNT showed better stability, reproducibility and linear range compared with NCNT, and it also had good interference immunity. In addition, the results of this entecavir electrochemical sensor were satisfactory in the detection of real samples, and it is expected to be applied to the detection of entecavir.

References

1. C. Srisomwat, A. Yakoh, N. Chuaypen, P. Tangkijvanich, T. Vilaivan, O. Chailapakul, *Anal. Chem.*, 93 (2021) 2879–2887.
2. Y. Tao, K. Yi, H. Wang, K. Li, M. Li, *Sens. Actuators B Chem.*, 361 (2022) 131711.
3. R.A. de Almeida Pondé, *Microbiol. Immunol.*, 66 (2022) 1–9.
4. R.A. de A. Pondé, *Arch. Virol.*, 164 (2019) 2645–2658.
5. Y. Lu, Y. Lin, Z. Zheng, X. Tang, J. Lin, X. Liu, M. Liu, G. Chen, S. Qiu, T. Zhou, *Biomed. Opt. Express*, 9 (2018) 4755–4766.
6. S. Dave, S. Park, M.H. Murad, A. Barnard, L. Prokop, L.A. Adams, S. Singh, R. Loomba, *Hepatology*, 73 (2021) 68–78.
7. S.U. Kim, Y.S. Seo, H.A. Lee, M.N. Kim, Y.R. Lee, H.W. Lee, J.Y. Park, D.Y. Kim, S.H. Ahn, K.-H. Han, S.G. Hwang, K.S. Rim, S.H. Um, W.Y. Tak, Y.O. Kweon, B.K. Kim, S.Y. Park, *J. Hepatol.*, 71 (2019) 456–464.
8. G.V. Papatheodoridis, G.N. Dalekos, R. Idilman, V. Sypsa, F. Van Boemmel, M. Buti, J.L. Calleja, J. Goulis, S. Manolakopoulos, A. Loglio, M. Papatheodoridi, N. Gatselis, R. Veelken, M. Lopez-Gomez, B.E. Hansen, S. Savvidou, A. Kourikou, J. Vlachogiannakos, K. Galanis, C. Yurdaydin, R. Esteban, H.L.A. Janssen, T. Berg, P. Lampertico, *J. Hepatol.*, 73 (2020) 1037–1045.
9. C.-H. Tseng, Y.-C. Hsu, T.-H. Chen, F. Ji, I.-S. Chen, Y.-N. Tsai, H. Hai, L.T.T. Thuy, T. Hosaka, H. Sezaki, J.A. Borghi, R. Cheung, M. Enomoto, M.H. Nguyen, *Lancet Gastroenterol. Hepatol.*, 5 (2020) 1039–1052.
10. M. Shoaib, A. Naz, F.A. Osra, S.H. Abro, S.U. Qazi, F.A. Siddiqui, M.R. Shah, A.Z. Mirza, *Arab. J. Chem.*, 14 (2021) 102974.
11. S.L. Dalmora, M. da S. Sangoi, D.R. Nogueira, L.M. da Silva, *J. AOAC Int.*, 93 (2010) 523–530.
12. F.-J. Zhao, H. Tang, Q.-H. Zhang, J. Yang, A.K. Davey, J. Wang, *J. Chromatogr. B*, 881–882 (2012) 119–125.
13. A.M. Asran, M.A. Mohamed, N. Ahmed, C.E. Banks, N.K. Allam, *J. Mol. Liq.*, 302 (2020) 112498.
14. H. Vlčková, J. Janák, T. Gottvald, F. Trejtnar, P. Solich, L. Nováková, *J. Pharm. Biomed. Anal.*, 88 (2014) 337–344.
15. D. Zhang, Y. Fu, J.P. Gale, A.F. Aubry, M.E. Arnold, *J. Pharm. Biomed. Anal.*, 49 (2009) 1027–1033.
16. L. Nováková, T. Gottvald, H. Vlčková, F. Trejtnar, J. Mandíková, P. Solich, *Mass Spectrom. Innov. Appl. Part VII*, 1259 (2012) 237–243.
17. M. Gao, R. Lin, L. Li, L. Jiang, B. Ye, H. He, L. Qiu, *Spectrochim. Acta. A. Mol. Biomol. Spectrosc.*, 126 (2014) 178–183.
18. A.A. Elzaher, M.A. Fouad, O.M. Elhoussini, Y.E.-E. Behery, *Bull. Fac. Pharm. Cairo Univ.*, 54 (2016) 175–179.
19. A. Naz, I. Tabish, A. Naseer, A.Z. Siddiqi, F.A. Siddiqui, A.Z. Mirza, *Future J. Pharm. Sci.*, 7 (2021) 75.
20. H.M. El-Sayed, L.E. Abdel Fattah, H.E. Abdellatef, M.A. Hegazy, M.M. Abd El-Aziz, *J. AOAC Int.*, 104 (2021) 847–853.

21. B.R. Challa, B.Z. Awen, B.R. Chandu, S. Rihanaparveen, *J. Chromatogr. B*, 879 (2011) 769–776.
22. K. Jhankal, A. Sharma, D. Sharma, *J. Pharm. Sci. Res.*, 7 (2015) 10.
23. Q. Jiang, Y. Liu, Y. Wang, Y. Sun, B. Li, Z. Li, T. Lu, S. Wang, Z. He, *RSC Adv.*, 6 (2016) 70990–70998.
24. R.D. Tandel, R.S. Naik, J. Seetharamappa, *Electroanalysis*, 29 (2017) 1301–1309.
25. J. Lu, M. Cheng, C. Zhao, B. Li, H. Peng, Y. Zhang, Q. Shao, M. Hassan, *Ind. Crops Prod.*, 176 (2022) 114267.
26. J. Wang, X. Yan, Z. Zhang, H. Ying, R. Guo, W. Yang, W. Han, *Adv. Funct. Mater.*, 29 (2019) 1904819.
27. L. Liu, X. Zhang, F. Yan, B. Geng, C. Zhu, Y. Chen, *J. Mater. Chem. A*, 8 (2020) 18162–18172.
28. Y.-S. Liu, C. Ma, Y.-L. Bai, X.-Y. Wu, Q.-C. Zhu, X. Liu, X.-H. Liang, X. Wei, K.-X. Wang, J.-S. Chen, *J. Mater. Chem. A*, 6 (2018) 17473–17480.
29. T. Wu, M. Jing, Y. Liu, X. Ji, *J. Mater. Chem. A*, 7 (2019) 6439–6449.
30. Z. Zhan, Y. Li, Y. Zhao, H. Zhang, Z. Wang, B. Fu, W.J. Li, *Biosensors*, 12 (2022) 221.
31. H. Xie, G. Luo, Y. Niu, W. Weng, Y. Zhao, Z. Ling, C. Ruan, G. Li, W. Sun, *Mater. Sci. Eng. C*, 107 (2020) 110209.
32. J. Gao, H. Liu, C. Tong, L. Pang, Y. Feng, M. Zuo, Z. Wei, J. Li, *Sens. Actuators B Chem.*, 307 (2020) 127628.
33. G.-C. Han, X. Su, J. Hou, A. Ferranco, X.-Z. Feng, R. Zeng, Z. Chen, H.-B. Kraatz, *Sens. Actuators B Chem.*, 282 (2019) 130–136.